

# Study of traps in polydiacetylene based devices using TSC technique\*

C. Renaud<sup>1,a</sup>, C.H. Huang<sup>1,2</sup>, M. Zemmouri<sup>1</sup>, P. Le Rendu<sup>1</sup>, and T.P. Nguyen<sup>1</sup>

<sup>1</sup> Université de Nantes, Institut des Matériaux Jean Rouxel, 2 rue de la Houssinière, 44332 Nantes Cedex 3, France

<sup>2</sup> Department of Applied Chemistry, National Chiao Tung University, Hsinchu 300, Taiwan

Received: 25 July 2006 / Accepted: 6 October 2006  
Published online: 6 December 2006 – © EDP Sciences

**Abstract.** Trap parameters in poly(1-(3,4-difluorophenyl)-2-(4-pentylcyclohexylphenyl)acetylene) (PDPA-2F) based devices have been investigated by using the thermally stimulated current (TSC) technique. The device structure is ITO-PEDOT-(PDPA-2F)-M, where M stands for the cathode metal (Al, Ca/Al, and Au). The results reveal at least three TSC peaks in devices denoted as peaks A, B and C. Comparing trap parameters in ITO-PEDOT-(PDPA-2F)-Au hole-only device and ITO-PEDOT-(PDPA-2F)-Ca Al (Al) bipolar devices, we assigned A and B trap types to hole-like traps and C type traps to electron-like traps. The trap densities are in the range of  $10^{15}$ – $10^{17}$  cm<sup>-3</sup> and the trap levels are 0.12 eV (A type traps), 0.36 eV (B type traps), and 0.25 eV (C type traps).

**PACS.** 72.20.Jv Charge carriers: generation, recombination, lifetime, and trapping – 72.80.Le Polymers; organic compounds (including organic semiconductors) – 81.05.Lg Polymers and plastics; rubber; synthetic and natural fibers; organometallic and organic materials – 85.60.Jb Light-emitting devices

## 1 Introduction

The electrical properties of semiconductors are governed in a large degree by defects or impurities incorporated, intentionally or not, to the materials during synthesis processes. In the field of organic materials and polymers, the presence of defects or traps influences strongly the transport of charge carriers through the materials, and hence the performances of devices using them as an active layer. Despite intensive investigations on electrical and optical properties of different materials [1–6], the formation process of defects in organic semiconductors is still not very well understood. In fact, there are two possibilities for creating defects in organic materials. They can result either from chemical impurities introduced to the materials or from different mechanisms such as oxidation, reduction, chain breaking... modifying the structure of the semiconductors.

For investigating traps in organic materials, both optical [7–9] and electrical [10–15] techniques can be used to obtain information of the trap parameters such as activation energy, density, capture cross section...

In this work, we have investigated trap parameters in a derivative of polyacetylene: poly[(1-(3,4-difluorophenyl)-2-(4-pentylcyclohexylphenyl) acetylene)] (PDPA-2F) by using the thermally stimulated current (TSC) technique.

This polymer is a new polydiphenylacetylene material having fluorine atoms on the backbone, which are expected to provide high electron mobility, and thus better transport properties than those previously studied. Different cathode configurations of PDPA-2F diode based devices have been investigated in order to check the influence of the polymer-electrode interface on the trap formation. The results will be discussed in relation with the electrical characteristics of the devices.

## 2 Experimental

PDPA-2F, synthesized by a method previously reported [16] was dissolved in toluene with concentration of 6 mg/mL. Indium tin oxide (ITO) coated glass substrates were cleaned in successive ultrasonic baths of distilled water, ethanol and acetone. After drying in nitrogen atmosphere, the substrates were treated by UV ozone before use. A thin layer (40–50 nm) of polyethylene dioxythiophene: polystyrene sulfonate (PEDOT:PSS) was deposited on the ITO substrate, which was then annealed at 150 °C for one hour under vacuum. The polymer film of thickness about 70–80 nm was spin-coated onto the PEDOT-PSS film, and the fabrication of the device was achieved with deposition of a cathode (Ca/Al, Al, Au) under high vacuum conditions ( $<10^{-6}$  mbar). The devices were encapsulated with a glass cover lit using an epoxy resin. The structure of the studied devices is ITO/PEDOT:PSS/PDPA-2F/CaAl (Al, Au).

\* This paper has been presented at “ECHOS06”, Paris, 28–30 juin 2006.

<sup>a</sup> e-mail: cedric.renaud@cnsr-imm.fr

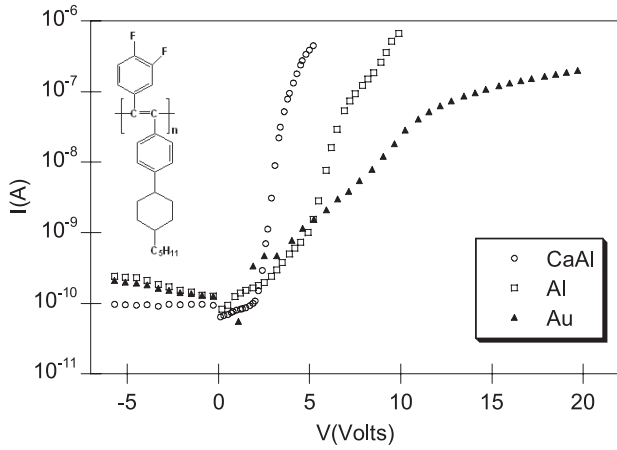


**Fig. 1.** Current-voltage characteristics of ITO/PEDOT/PDPA-2F/metal devices at  $T = 300$  K, with different anode metals.

The TSC experiments were carried using a cryostat whose temperature was controlled by an Oxford 503 unit. A Keithley 230 programmable voltage source coupled with a Keithley 617 electrometer was used for monitoring the TSC spectra. The measurement procedure is as follows. At high temperature  $T_H$ , a voltage  $V_H$  is applied to the device during a charging time  $t_C$  of 5 minutes. The sample is then cooled to low temperature  $T_L$  with applied voltage  $V_H$  and then is short-circuited. After being allowed to reach an equilibrium state, the sample is heated at constant heating rate  $\beta = dT/dt$ , and the current is recorded as function of the temperature, giving the TSC spectrum. By modifying the charging voltage  $V_H$ , one can expect to observe the charge released from the electron or the hole traps depending on the polarity of the sample.

### 3 Results and discussion

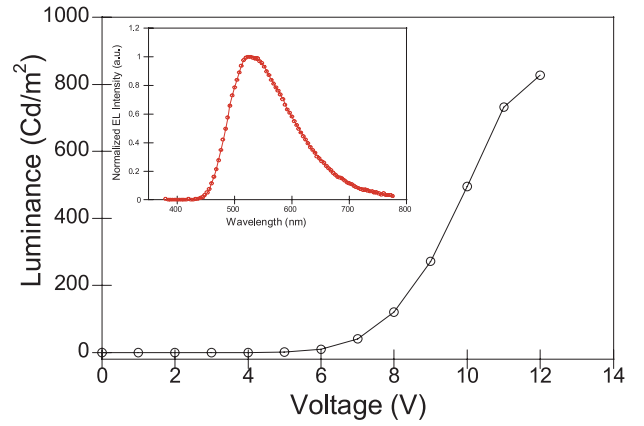
#### 3.1 Current-voltage and luminance characteristics

Figure 1 shows the current-voltage characteristics at  $T = 300$  K for three similar diodes but having different cathodes: ITO/PEDOT/PDPA-2F/CaAl (device 1), ITO/PEDOT/PDPA-2F/Al (device 2) and ITO/PEDOT/PDPA-2F/Au (device 3) respectively.

A strong dependence of the current density on the nature of the cathode is observed. In Figure 2, the electro-luminescence characteristics of device 1 are shown. The photoluminescence spectrum of the polymer shows a peak at 536 nm with a green-yellow light. On the other hand, a maximum luminance of 827  $\text{cd/m}^2$  at 12 V is obtained and a maximum current efficiency of 0.78  $\text{cd/A}$  at 9 V with a current density of  $\sim 35$   $\text{mA/cm}^2$ .

#### 3.2 TSC measurements

The TSC peaks arise from the increased number of free carriers, which are released thermally by de-trapping.



**Fig. 2.** Luminance-voltage characteristic of ITO/PEDOT/PDPA-2F/CaAl diode at  $T = 300$  K. Inset is the electro-luminescence spectrum of device at  $T = 300$  K.

Therefore, the temperature at which a current peak occurs is correlated to energetic depth of the trap states. By integrating the released current over time, the amount of trapped charges  $\Delta Q$  is obtained and the average trap density  $N_t$  can be evaluated by the following relation:

$$N_t = \frac{\Delta Q}{eAd} \quad (1)$$

where  $e$  is the electronic charge,  $A$  is the surface, and  $d$  is thickness of the sample.

Assuming that re-trapping of released charge carriers is negligible and that the probability for a carrier to escape from a trap obeys to Boltzmann statistic, Cowell and Woods [17] derived the following relation for TSC:

$$I(T) = N_{t0} \cdot s \cdot \exp\left(-\frac{E_t}{kT}\right) \times \exp\left(-\frac{s}{\beta}\right) \int_{T_0}^T \exp\left(-\frac{E_t}{kT'}\right) dT' \quad (2)$$

where  $N_{t0}$  and  $T_0$  are the initial concentration and temperature of trapped charge carrier respectively,  $k$  is the Boltzmann constant,  $s$  is the frequency factor,  $T$  is the absolute temperature and  $E_t$  is the activation energy.

The TSC maximum temperature  $T_m$  is given by the following relation:

$$\frac{\beta E_t}{kT_m^2} = s \cdot \exp\left(-\frac{E_t}{kT_m}\right). \quad (3)$$

The “initial rise” method is based on the assumption that when traps begin to empty as the temperature increased. Therefore, for temperatures lower than  $T_m$ , the TSC is proportional to  $\exp(-E_t/kT)$  [18]. Thus a plot of the logarithm of current flow versus  $1/kT$  yields a straight line with a slope of  $E_t$ . Equations (1–3) are used for determining the different trap parameters from experimental data. Figure 3 shows the TSC spectra of a

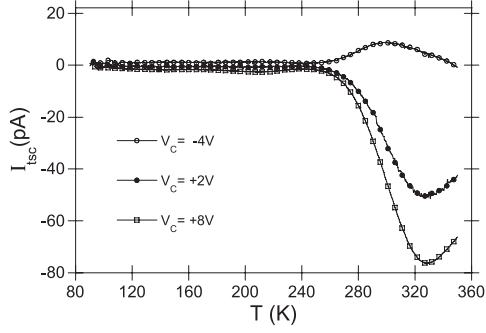


**Fig. 3.** TSC spectra recorded in a ITO/PEDOT/PDPA-2F/Au diode using the following parameters:  $T_H = 300$  K,  $\beta = 3$  K/min, with different charging voltages:  $V_C = -4$  V,  $V_C = +2$  V,  $V_C = +8$  V.

**Table 1.** Summary of the trap parameters in ITO/PEDOT/PDPA-2F/Au diodes.

Peak	$V_H$ (Volts)	$\beta$ (K/s)	$E_a$ (eV)	$N_t$ ( $\text{cm}^{-3}$ )
A	+8	0.05	0.12	$1 \times 10^{16}$
B	+8	0.05	0.36	$2 \times 10^{17}$

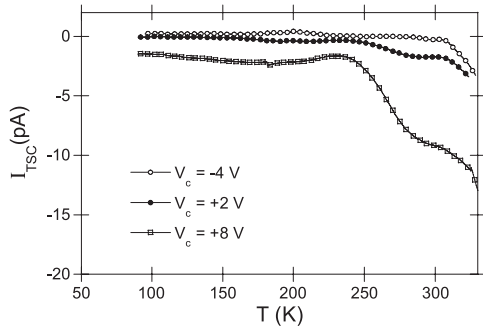


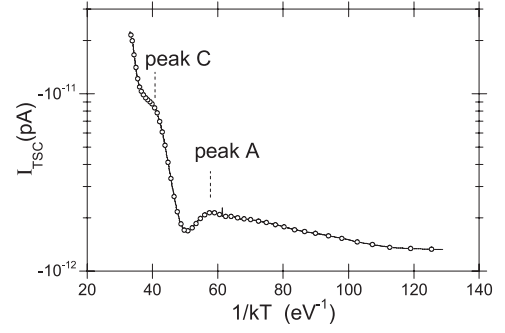
**Fig. 4.** TSC spectra recorded in a ITO/PEDOT/PDPA-2F/CaAl diode using the following parameters:  $T_H = 300$  K,  $\beta = 3$  K/min, with different charging voltages:  $V_C = -4$  V,  $V_C = +2$  V,  $V_C = +8$  V.

ITO/PEDOT:PSS/PDPA-2F/Au diode (device 3) at different biases. The characteristic is strongly asymmetrical. With a positive applied voltage (forward direction), the TSC spectrum shows two peaks located at 210 (peak A) and 328 K (peak B) respectively.

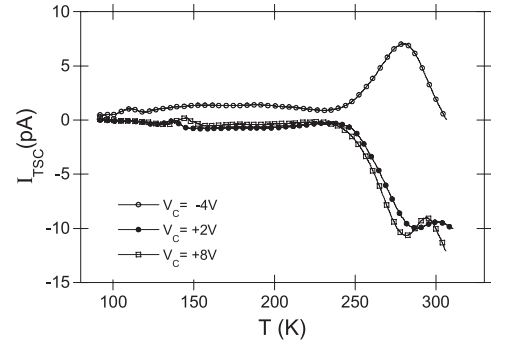
With a negative applied voltage (reverse direction), while the low temperature peak (A) is similar (207 K) to that previously obtained, the high temperature peak (B) is found at 300 K, with a weaker intensity. Their nature will be discussed below with the results obtained in devices using Al and CaAl cathodes. The parameters corresponding to the two peaks are reported in Table 1.

Figure 4 shows the TSC spectra of a ITO/PEDOT:PSS/PDPA-2F/CaAl at different charging voltages.

To distinguish between TSC and spurious current peaks, the logarithm of current versus  $1/kT$  was plotted



**Fig. 5.** Logarithm of TSC current vs.  $1/kT$  for a ITO/PEDOT/PDPA-2F/CaAl diode using the following parameters:  $T_H = 300$  K,  $\beta = 3$  K/min,  $V_C = +8$  V.



**Fig. 6.** TSC spectra recorded in a ITO/PEDOT/PDPA-2F/CaAl diode using the following parameters:  $T_H = 300$  K,  $\beta = 3$  K/min, with different charging voltages:  $V_C = -4$  V,  $V_C = +2$  V,  $V_C = +8$  V.

as shown in Figure 5. Only true TSC peaks appear while spurious currents do not show observable peaks.

Figure 6 shows the TSC spectra of a ITO/PEDOT:PSS/PDPA-2F/Al at different charging voltages. We note that peak A remains similar to that observed in device with a gold cathode, suggesting that the corresponding trap states are independent of the electrode configuration, and consequently are bulk traps. On the other hand, a new peak (C) is found at 285 K in both reverse and forward directions for device using Al cathode. This peak is observed in forward direction only for device using CaAl cathode. The peak position and the activation energy of peak C ( $\sim 0.25$  eV) indicate that this peak is not a shift of peak B observed in device 3. Furthermore, at high temperature ( $>300$  K) we note the onset of an additional peak whose activation energy is  $\sim 0.36$  eV as determined by the initial rise evaluation technique.

Device 3 (ITO/PEDOT:PSS/PDPA-2F/Au) with high work function cathode ( $\psi_{\text{Au}} = 5.2$  eV) is a “hole-only” one, and does not emit light. Charge carriers that are injected into the polymer layer are essentially holes, and the trapped charges observed in the TSC spectra correspond to hole-like traps. This observation implies that peaks A and B are hole traps in PDPA-2F.

Devices 1 (CaAl cathode) and 2 (Al cathode) are bipolar with light emission. In these devices, under a sufficient

bias, electrons are injected from the cathode because the barrier height at the interface is less than that of the device 3. The similarity of the peak C in position and activation energy in both devices suggests that the corresponding traps are electron-like traps. As for the traps observed in the temperature range higher than 300 K in these devices, they would correspond to the B type traps found in device 1 because they have comparable energy level. Contrarily to peak B, which is symmetrical with regards to the polarity of sample 2, peak C has lower intensity in reverse bias condition as compared to that obtained with a forward applied voltage. In fact, at high temperature the TSC spectrum shows a reverse current (in the sense of the charging current). This current reversal has been observed in several polymer-based devices [19,20] and can be related to the properties of the interface between the polymer and the cathode [19]. An evident dependence of this peak on the nature of the electrode (Al and CaAl) suggests that the corresponding traps are in the vicinity of the cathode.

The results obtained in this work can be compared to those previously reported in polymer based diodes using TSC technique for studying trapping process [21–25]. It should be noted that contradictory results on trap determination have been reported in similar polymers, indicating that the preparation of the samples has a prime influence on the trap parameters. Typical illustrations are PPV [21,22] and MEH-PPV [23,24] studies for which not only trap levels but also trap types differ from different investigations. In the case of poly(2-methoxy-5-(3',7'-dimethyloctyloxy)-1,4-phenylene vinylene) or OC<sub>1</sub>C<sub>10</sub>, a systematical study using bipolar, hole only and electron only devices could distinguish between hole and electron traps, providing a detailed description of traps in this polymer [25]. Trap densities of  $\sim 10^{15}$  cm<sup>-3</sup> were found which are comparable to values determined in our work. The difference between the results of [25] and ours is the following. With a reverse bias applied, no TSC was observed in OC<sub>1</sub>C<sub>10</sub> diodes, while in our devices, TSC peaks were observed. Both electron and hole trapping occurred with much less trapped carriers as compared to the forward condition experiments. Possible explanation is the imperfect contacts between polymer and electrodes allow residual charge injection and consequently their trapping. The reverse current does not equal zero in all samples. In the sample with CaAl electrode, no electron trapping was observed in the TSC spectrum when the device was negatively biased (Fig. 4). This observation can be explained by the possible oxidation of calcium layer after its deposition, making injection of electrons less efficient.

## 4 Conclusion

Thermally Stimulated Current technique has been used to investigate electrically active traps in disubstituted polyacetylene based diodes. The device emits green-yellow light with a good luminance that can be potentially exploited in display fabrication. Analysis of TSC spectra shows that both hole and electron traps could be iden-

tified. Hole trap levels are found at  $\sim 0.1$  and  $0.4$  eV from the HOMO with density of  $\sim 5 \times 10^{15}$  and  $1 \times 10^{17}$  cm<sup>-3</sup> respectively. Electron traps are located at  $\sim 0.30$  eV from the LUMO level with a density of  $\sim 1 \times 10^{16}$  cm<sup>-3</sup>. The electron traps seem to strongly depend on nature of the polymer-cathode interface, and are expected to locate in the vicinity of the interface region.

## References

1. E.J.W. List, C.H. Kim, J. Shinar, A. Pogantsch, G. Leising, W. Graupner, Appl. Phys. Lett. **76**, 2083 (2000)
2. Y. Hashimoto, T. Kawai, M. Takada, S. Maeta, M. Hamagaki, T. Sakakibara, Jpn J. Appl. Phys. **42**, 5672 (2003)
3. V. Kumar, S.C. Jain, A.K. Kapoor, W. Greens, T. Aernauts, J. Poortmans, R. Mertens, J. Appl. Phys. **94**, 1283 (2003)
4. N. von Malm, R. Schmechel, H. von Seggern, SID Symposium Digest **34**, 1072 (2003)
5. I. Tanaka, S. Tokito, Appl. Phys. Lett. **87**, 173509 (2005)
6. H.E. Tseng, C.Y. Liu, S.A. Chen, Appl. Phys. Lett. **88**, 042112 (2006)
7. M. Yan, L.J. Rothberg, F. Papadimitrakopoulos, M.E. Galvin, T.M. Miller, Phys. Rev. Lett. **73**, 744 (1990)
8. R.N. Marks, M. Muccini, E. Lunedi, R.H. Michel, M. Murgia, R. Zamboni, C.Taliani, G. Horowitz, F. Garnier, M. Hopmeier, Oestrich, R.F. Mahrt, Chem. Phys. **227**, 49 (1998)
9. S. Trabatttoni, S. Laera, R. Mena, A. Papagni, A. Sassella, J. Mater. Chem. **14**, 171 (2004)
10. A.J. Campbell, D.D.C. Bradley, D.G. Lidzey, J. Appl. Phys. **82**, 1961 (1997)
11. J. Scherbel, P.H. Nguyen, G. Paasch, W. Brütting, M. Schwoerer, J. Appl. Phys. **83**, 5045 (1998)
12. M. Onoda, D.H. Park, K. Yoshino, J. Phys.-Cond. Mat. **1**, 113 (1989)
13. S. Karg, J. Steiger, H. Von Seggern, Synthetic Met. **111**, **112**, 277 (2000)
14. A.J. Campbell, D.D.C. Bradley, E. Werner, W. Brütting, Synthetic Met. **111**, **112**, 273 (2000)
15. O. Gaudin, R.B. Jackman, T.P. Nguyen, P. Le Rendu, J. Appl. Phys. **90**, 4196 (2001)
16. C.H. Ting, C.S. Hsu, Jpn J. Appl. Phys. **40**, 5342 (2001)
17. T.A.T. Cowell, J. Woods, Brit. J. Appl. Phys. **18**, 1045 (1967)
18. K.H. Nicholas, J. Woods, Brit. J. Appl. Phys. **15**, 783 (1965)
19. J. Van Turnhout, *Thermally Stimulated Discharge of Polymer Electrets* (Elsevier, Amsterdam, 1975)
20. A. Samoc, M. Samoc, J. Sworakowski, Phys. Status Solidi A **39**, 337 (1977)
21. T.P. Nguyen, V.H. Tran, V. Massardier, J. Phys.-Cond. Mat. **5**, 6243 (1993)
22. M. Meier, S. Karg, K. Zuleeg, W. Brütting, M. Schwörer, J. Appl. Phys. **84**, 87 (1998)
23. A.A. Alagiriswamy, K.S. Narayan, Synthetic Met. **116**, 297 (2001)
24. V. Kazukauskas, H. Tzeng, S.A. Chen., Appl. Phys. Lett. **80**, 2017 (2002)
25. N. von Malm, J. Steiger, H. Heil, R. Schmechel, H. von Seggern, J. Appl. Phys. **92**, 7564 (2002)